Regular Article

INORGANIC CHEMISTRY RESEARCH
Published by the
Iranian Chemical Society
www.inorgchemres.org
info@inorgchemres.org

Inorg. Chem. Res., *Vol. 5, No. 1, 149-162, June 2021*
DOI: 10.22036/icr.2021.259897.1097

Conversion of Levulinic Acid to *n*-Butyl Levulinate over Mesoporous Zirconium Phosphate Catalysts

Fatemeh Jamali, Alireza Najafi Chermahini* and Neda Ayashi
Department of Chemistry, Isfahan University of Technology, 84154-83111 Isfahan, Iran
(Received 30 November 2020, Accepted 27 February 2021

In this study, mesoporous zirconium phosphates (m-ZrPs) with a different molar ratio of phosphate to zirconium were synthesized and used as the heterogeneous catalyst for the production of n-butyl levulinate from levulinic acid. The catalysts were characterized using various techniques such as N_2 adsorption-desorption, XRD, FT-IR, ICP-OES, SEM and TEM. The prepared catalysts were confirmed to possess the mesoporous structure with a high surface area. Among the synthesized catalysts, m-ZrP-2 showed the best performance in the conversion of levulinic acid to n-butyl levulinate. The reaction conditions were optimized on parameters such as reaction time, temperature, amount of catalyst, and the molar ratio of LA to n-butanol. Temperature 120 °C, reaction time 7 h, the ratio of acid to alcohol 1:9 and 0.01 g catalyst were selected as the optimum conditions. In addition, the selected m-ZrP-2 catalyst was successfully recycled for six consecutive cycles without significant loss in its activity.

Keywords: Levulinic acid, Butyl levulinate, Mesoporous zirconium phosphate, Esterification, Biomass conversion

INTRODUCTION

In recent decades, the huge consumption of fossil fuels has led to a reduction in energy reserves, as well as an increase in greenhouse gas emissions and the subsequent increase in global temperature. Therefore, the replacement of fossil fuels with renewable sources such as wind, biomass, solar, *etc*., is of particular interest [1]. Biomass is the only carbon-based renewable resource used to manufacture platform building blocks for the production of chemicals and liquid fuels [2,3]. Levulinic acid (LA), 5-hydroxy-methylfurfural (5-HMF), and furfural are the key chemical platforms that can be synthesized from biomass [3,4].

Levulinic acid (LA) (also known as 4-oxopentanoic acid or g-ketovaleric acid) is one of the most promising chemicals which can be produced directly by acid hydrolysis of lignocellulosic biomass [5,6]. The importance of levulinic acid is due to the presence of two functional groups of ketone and carboxylic acid and can be converted into various important derivatives such as alkyl levulinates, γ-valerolactone, 2-methyl tetrahydrofuran, succinic acid and alkyl 4-alkoxypentanoates [7,8]. Esterification reaction between levulinic acid and alcohols in the presence of a suitable acid catalyst leads to alkyl levulinates (AL). Low toxicity, high flash point, high boiling point, low vapor pressure, and low viscosity, making ALs attractive alternatives to petrol and diesel fuels [9,10]. ALs are the main precursor in the production of biofuel additives, solvents, pesticides, plasticizers, and polymers [11-13]. Generally, the conversion of LA into AL is catalyzed by mineral acids such as HCl, H_2SO_4 and heterogeneous catalysts. Liquid mineral acid catalysts are corrosive and destroy industrial and experimental equipment. In addition, it is difficult to separate them, which leads to the release of hazardous residues [14,15]. Therefore, the use of heterogeneous catalysts is of interest because they can be easily separated and reused and also are not corrosive to the reactor materials [16]. Heteropoly acids (HPAs), zeolites,

*Corresponding author. E-mail: anajafi@iut.ac.ir

resin catalysts and metal-organic frameworks (MOFs) are the common heterogeneous acid catalysts, which are used to synthesis alkyl levulinates from levulinic acid [17-22].

Mesoporous catalysts are potential catalysts for the synthesis of organic compounds that have attracted the attention of many researchers in recent years because of their narrow and uniform pore size distribution, high surface area, tunable pore size, and high thermal stability [23-29]. Zirconium exchanged phosphotungstic acid, sulfonated carbon catalysts, SBA-15-Pr-SO_3H, aluminum-containing MCM-41, mesoporous stannosilicates SnTUD-1 and mesoporous titanium dioxide functionalized by organosilica hybrid catalysts, are mesoporous catalysts used in the preparation of alkyl levulinates [30-35]. Mesoporous zirconium phosphate is used as a heterogeneous catalyst because of its superior surface area (>300 m^2 g^{-1}), distribution of narrow pore size, high thermal stability up to 800 °C, easy sedimentation, and appropriate acidity [36]. The use of the m-Zr-P catalyst has been reported for ester hydrolysis, alcohol dehydration and Friedel-Crafts alkylation, Fischer esterification, synthesis of coumarin derivatives, and synthesis of 5-hydroxymethylfurfural [37-39].

Considering the importance of alkyl levulinates and the increasing need to develop a novel and simple method for their production, and in the continuation of our studies on the synthesis of alkyl levulinates [32-34], we herein wish to describe an efficient synthesis of butyl levulinate from levulinic acid catalyzed by mesoporous zirconium phosphate with the different molar ratio of phosphate to zirconium as heterogeneous catalysts which have a reasonable amount of Lewis and Brönsted acid sites. The synthesized catalysts were characterized by different methods such as nitrogen adsorption-desorption analysis, XRD, FTIR, FESEM, EDS and TEM techniques. To find the optimum reaction conditions, a series of parameters such as reaction time, reaction temperature, loading of catalyst, and acid:*n*-butanol ratio were investigated. For more evaluation of effect phosphate adduct as well as the textural properties of synthesized catalysts, zirconium oxide was synthesized and its catalytic activity was compared in the esterification reaction.

EXPERIMENTAL

Materials and Methods

Zirconium(IV) oxide chloride octahydrate (>99%), ammonium carbonate, diammonium hydrogen phosphate (>99%), n-butanol (>99%), and toluene (>99%) were obtained from Merck, cetyltrimethylammonium bromide (CTAB, >99%) was obtained from Daejung (S. Korea), levulinic acid (>98%) was obtained from Acros, hydrogen peroxide (≥30%) was obtained from Ameretat Shimi (Iran).

Synthesis of Mesoporous Zirconium Phosphate

In this study, the ZrO_2 and m-ZrPs with the different molar ratio of phosphate to zirconium (1.5, 2.0, 2.5) were synthesized and marked as m-ZrP-x, which x: shows the molar ratio of phosphate to zirconium (P/Zr). m-ZrPs were synthesized based on the Sinhamahapatra *et al.* method [39]. In a typical synthesis, 8.00 g (0.02 mol) zirconium oxychloride.$8H_2O$ was dissolved in 100 mL of deionized (DI) water. A solution of ammonium carbonate was added dropwise to the zirconium oxychloride solution under continuous stirring, a white precipitate appeared. The mixture was filtered off and washed with DI water to remove the chloride ions. The obtained white solid was added to a solution of ammonium carbonate 5.00 g dissolved in 175 mL DI in a closed glass reactor. Then to this solution, was added 6.55 g (0.05 mol) di-ammonium hydrogen orthophosphate dissolved in 50 mL DI water and the mixture stirred for 20 min. To this solution was added 2.25 g (0.006 mol) cetyltrimethylammonium bromide (CTAB) and the whole reaction mixture was stirred for 12 h. Then the closed glass reactor was put at 80 °C for 2 days, at 90 °C for 1 day, and at 120 °C for 1 additional day. After cooling, the reaction mass was filtered, washed thoroughly with DI water, and was dried in the oven at 80 °C. Finally, the sample was calcined at 550 °C for 6 h to obtained mesoporous zirconium phosphate.

Synthesis of Zirconium Dioxide

5.00 g (0.016 mol) zirconium oxychloride octahydrate was dissolved in deionized water. A solution of sodium hydroxide (1.00 M) was added dropwise to the zirconium oxychloride solution under continuous stirring, a white

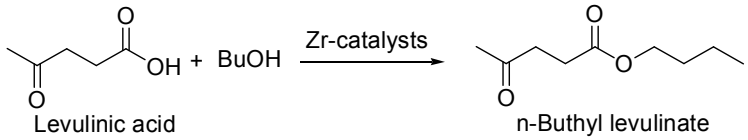

Scheme 1. Esterification LA with n-butanol

precipitate appeared. The mixture was filtered off and washed with DI water to remove the chloride ions. The sample after drying was calcined at 550 °C for 6 h to obtained zirconium dioxide.

Characterization

To analyze the functionalities of synthesized materials, Fourier Transforms Infrared Spectroscopy (JASCO FT/IR-680 PLUS, Japan) was used in the range of 400-4000 cm^{-1} by KBr pellet. An inductively coupled plasma spectrometry (ICP, model: Optima 7300DV) was applied to determine the amount of Zirconium and phosphorous in the synthesized catalysts. A transmission electron microscope (TEM, model: Philips CN120) was used for investigating the surface morphology of the synthesized samples. Field Emission Scanning Electron Microscopy (FESEM) analysis was performed on an FEI QNANTA 450 to obtain the micrographs of the samples. Also, energy dispersive X-ray spectroscopy (EDX) was used in connection with SEM for elemental analysis. The high angle powder X-ray diffraction (XRD) patterns of the catalysts were obtained on an Asenware XDM-300 diffractometer using Ni-filtered Cu Ka (K¼ 0.15406 nm) radiation. The Brunauer-Emmett-Teller (BET) specific surface area, pore-volume, and pore size distribution of the samples were measured using N_2 adsorption-desorption isotherms at the liquid-nitrogen temperature (77 K) on a PHS-1020 (PHS CHINA) apparatus. The type and quantity of the acid sites of the catalysts were determined by analysis of FT-IR spectra of adsorbed pyridine based on the following technique: A quantity of catalyst powder was pressed to a pellet, and in order to eliminate the moisture adsorbed on the surface of the catalyst, the pellet was heated at 120 °C for 2 h, and its FT-IR spectrum was taken. Then, pyridine adsorption was performed by adding a little pyridine into the pellet. After placing the pellet at room temperature for 24 h, the unreacted pyridine was desorbed by heating the pellet under vacuum at 120 °C for 2 h. Finally, the FTIR spectrum of the pyridine adsorbed on the catalyst pellet was taken at room temperature. According to the obtained spectra, acid site concentrations were calculated by Emeis equations [40].

Catalytic Esterification of LA with n-Butanol

In this investigation, mesoporous zirconium phosphate has been used as a solid acid catalyst in the conversion of LA to BL (Scheme 1). In a typical experiment, the reaction was carried out in a Teflon lined 25 mL autoclave by charging 0.5 mL LA (0.572 g), 4.5 mL *n*-butanol (3.645 g), and 0.05 g catalyst m-ZrPs which was magnetically stirred (1000 rpm) at the different temperature and reaction time. After running the reaction for a specified time, the mixture was cooled to room temperature and the heterogeneous catalyst was separated from the reaction mixture by filtration. The sample reaction was analyzed by GC (GC-2552, TGF Co.). The structure of the synthesized product was defined by gas chromatography (6890N Agilent Technologies) using a mass detector (Agilent Technologies).

RESULTS AND DISCUSSION

Catalyst Characterization

FT-IR spectroscopy. FTIR spectra of synthesized m-ZrPs (Fig. S1) show absorption bands at 1000-1100 cm^{-1} corresponding to P-O stretching vibration and bands at 2360 cm^{-1} due to the (P)-OH stretching vibration [41]. The bands at 3434 and 1637 cm^{-1} correspond to the asymmetric OH stretching and bending of the adsorbed water molecules, respectively. The band observed at 750 cm^{-1} relates to the P-O-P vibrations, which appears for the ratio 2.5, indicating the formation of polyphosphates. The band at 404 cm^{-1}, presents the O-P-O bending vibrations. The band at 520 cm^{-1} is due to Zr-O stretches of the zirconium oxide. The same

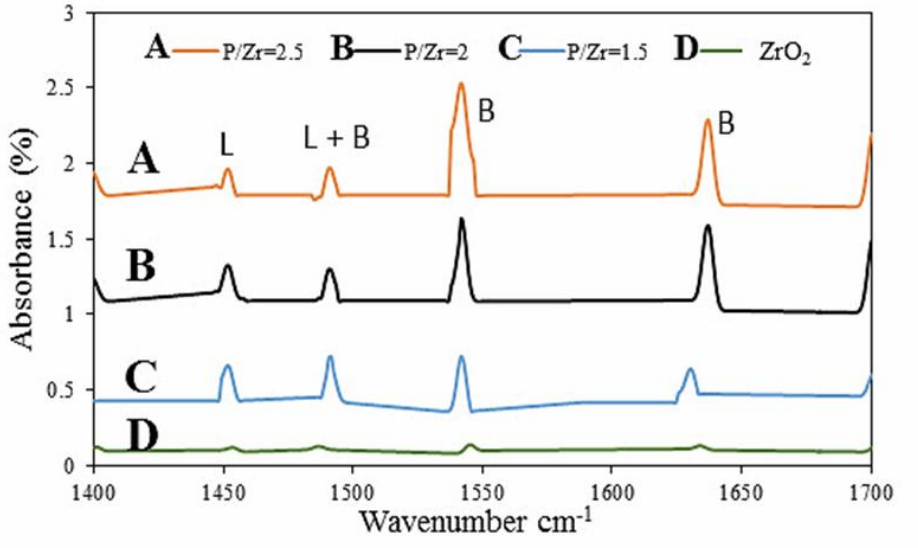

Fig. 1. FTIR spectra of pyridine adsorption for m-ZrPs and ZrO_2.

Table 1. Acidity Data of Solid Catalysts

Sample	Brönsted acid sites ($\mu mol\ g^{-1}$)	Lewis acid sites ($\mu mol\ g^{-1}$)	Total acidity ($\mu mol\ g^{-1}$)
ZrO_2	22.10	7.88	29.98
ZrP-1.5	292.93	121.04	413.97
ZrP-2	343.19	86.51	429.70
ZrP-2.5	360.12	60.33	420.45

peaks (3434, 1637 and 520 cm^{-1}) are seen in Fig. S1 for zirconium oxide. For the determination of the acidity of m-ZrPs and ZrO_2 compounds, the pyridine adsorption FT-IR spectroscopy was used as an effective method (Fig. 1). The strong bands at 1634 and 1541 cm^{-1} assigned to protonated pyridinium ions (Brönsted acid sites) which probably due to the presence of P (OH) and Zr (OH) groups [42]. The band at 1450 cm^{-1}, is the characteristic peak of Lewis acid centers. The band at 1494 cm^{-1} is a combination band between two separate bands at 1547 cm^{-1} and 1445 cm^{-1} corresponding to Brönsted and Lewis acid sites respectively. According to the results, m-ZrPs and ZrO_2 mesoporous, show both Brönsted acid and Lewis acid sites. The relative acid site concentration for catalysts, calculated from the integrated area of PyB (pyridine adsorption on Brönsted acid sites) and PyL (pyridine adsorption on Lewis acid sites) bands using the Emeis equations, are listed in Table 1.

XRD Patterns. Wide and small-angle powder XRD patterns of m-ZrPs are shown in Fig. 2. In addition, the wide-angle pattern of ZrO_2 is shown in Fig. S2. All catalysts display the usual band related to the amorphous mesoporous. Two broad peaks in 2θ ranges of 10-40° and 40-70° (Fig. 2A) in the wide-angle powder XRD patterns of m-ZrPs, indicate their amorphous nature. A single broad peak in

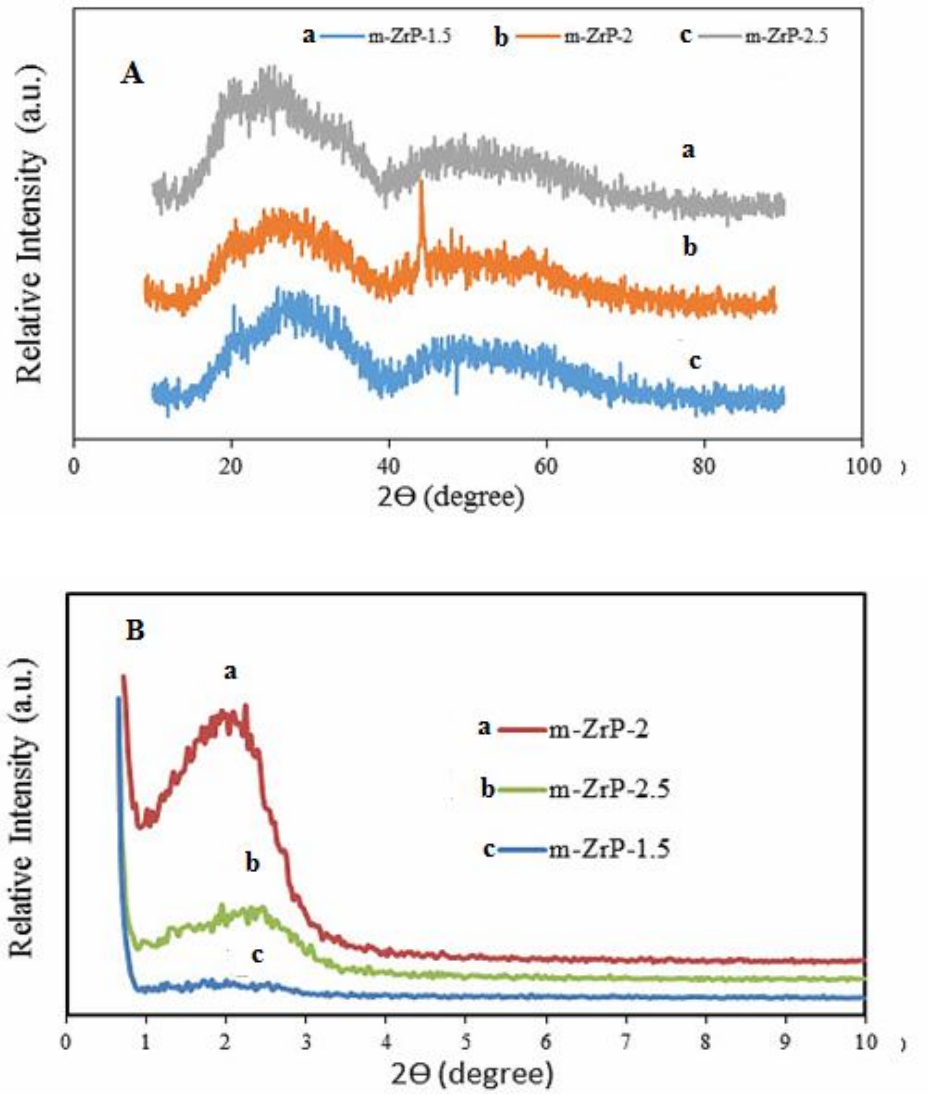

Fig. 2. Wide-angle (a) and small-angle (b) XRD patterns of synthesized m-ZrP.

small-angle powder XRD patterns of m-ZrPs is seen at around 2θ = 2.2-2.3 degree corresponding to a d-value of ~4 to 3.8 nm (Fig. 3b) [43]. The XRD pattern of bare zirconia is shown in Fig. S2 indicates diffractions characteristics for ZrO_2 structure suggesting the compound is successfully synthesized.

Nitrogen adsorption desorption analysis. The nitrogen adsorption-desorption isotherms of catalysts are given in Fig. 3. The patterns of all the samples correspond to type IV representing the mesoporous character of these catalysts [39]. Table 2 summarizes the textural properties like specific surface area (S_{BET}, m^2 g^{-1}), pore-volume, and pore size distribution. It is noteworthy that the BET surface area and pore volume of m-ZrPs decrease with increasing the phosphate to Zr molar ratio. Among all catalysts, ZrO_2 has the least BET surface area and pore volume and the largest pore size (4.63 nm).

Electron microscopy. The morphology of m-ZrPs and zirconia samples were evaluated by field emission scanning electron microscopy (FESEM) and transmission electron

Table 2. Textural Properties of m-ZrPs and ZrO_2

Sample	Cavities diameter (nm)	Total volume of cavities ($cm^3\ g^{-1}$)	Specific surface area ($m^2\ g^{-1}$)
ZrO_2	4.63	0.0366	15.6
ZrP-1.5	1.22	0.2426	366.1
ZrP-2	1.22	0.2266	306.4
ZrP-2.5	1.22	0.2026	262.0

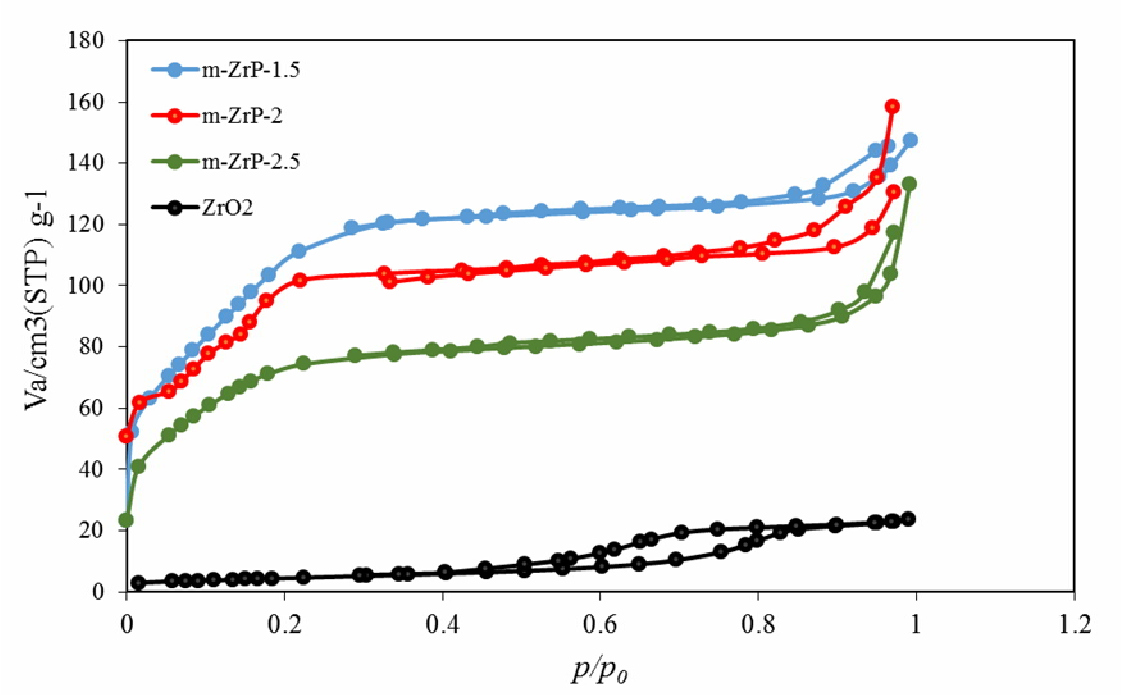

Fig. 3. Nitrogen adsorption-desorption isotherms of mesoporous zirconium phosphate samples.

microscopy (TEM). Figure S3 represents the scanning electron microscopy (SEM) images of the catalysts. SEM images show spherical particles with almost uniform sizes. The transmission electron microscopy (TEM) micrograph (Fig. 4) displays that all the spherical particles are connected and porous.

ICP Analysis. The inductively coupled plasma (ICP) analysis was used for elemental analysis of samples and it was confirmed that with the increase in di-ammonium hydrogen *ortho*phosphate as the phosphate source, the phosphorus amount increases in m-ZrPs catalysts from 2.71 to 3.73% (Table 3).

Catalytic Conversion of Levulinic Acid to n-Butyl Levulinate

Mechanism of the reaction. In the present study, three

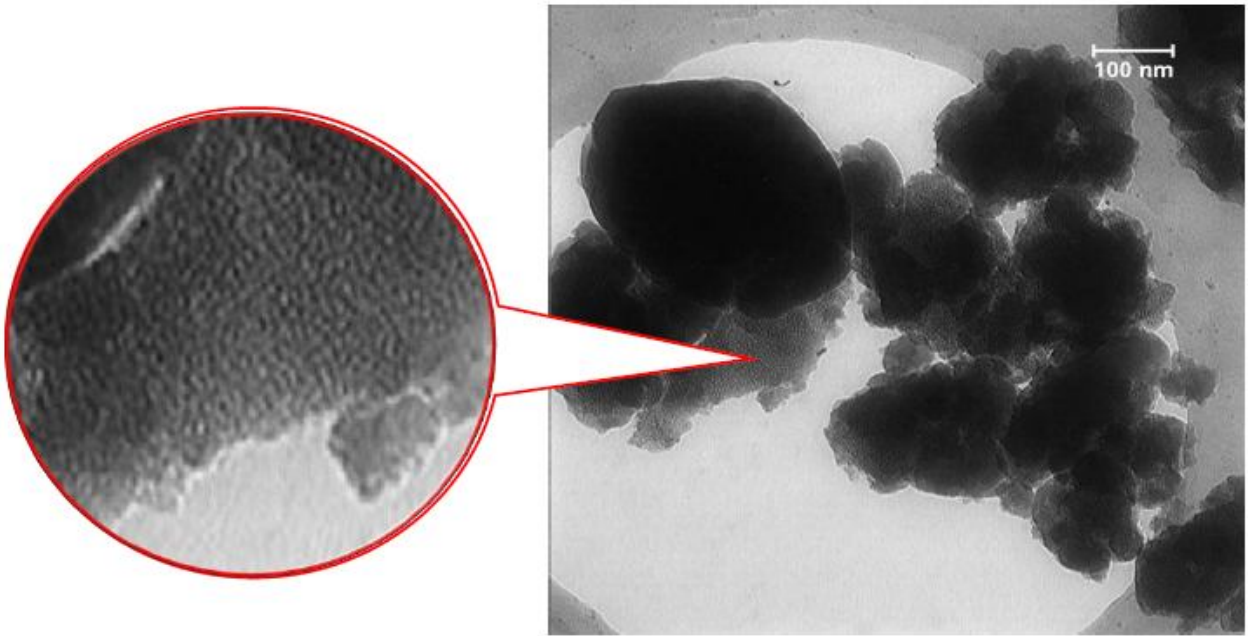

Fig. 4. TEM micrograph of m-ZrP-2 in different magnification.

Table 3. ICP Analysis Results of m-ZrPs and m-ZrO_2

Sample	Amount of phosphorus in the sample (w/w%)
m-ZrP-1	2.71
m-ZrP-2	3.20
m-ZrP-2.5	3.73
m-ZrP-2 recycled	1.54

types of mesoporous zirconium phosphate and zirconium oxide were synthesized and used for the conversion of levulinic acid to n-butyl levulinate. Both Lewis acid- as well as Brönsted acid-sites could be probably responsible for the conversion of levulinic acid to alkyl levulinate. On one hand, the carboxylic group of levulinic acid activated by Brönsted acid-sites of catalyst, which may undergo a nucleophilic attack of butanol and removal of a water molecule to afford the n-butyl levulinate (path A) (Scheme 2). From another point of view, zirconium as a Lewis acid site may facilitate the esterification reaction by activation of the carboxylic group (path B) (Scheme 2).

Effect of catalyst on the conversion of levulinic acid to n-butyl levulinate. The efficiency of various catalysts (m-Zrps (P/Zr = 1.5, 2, 2.50) and ZrO_2) in the conversion of levulinic acid to n-butyl levulinate was investigated at the temperature range of 90-120 ºC and reaction time of 2 to 7 h from the start of the reaction (Figs. 5 and 6). According

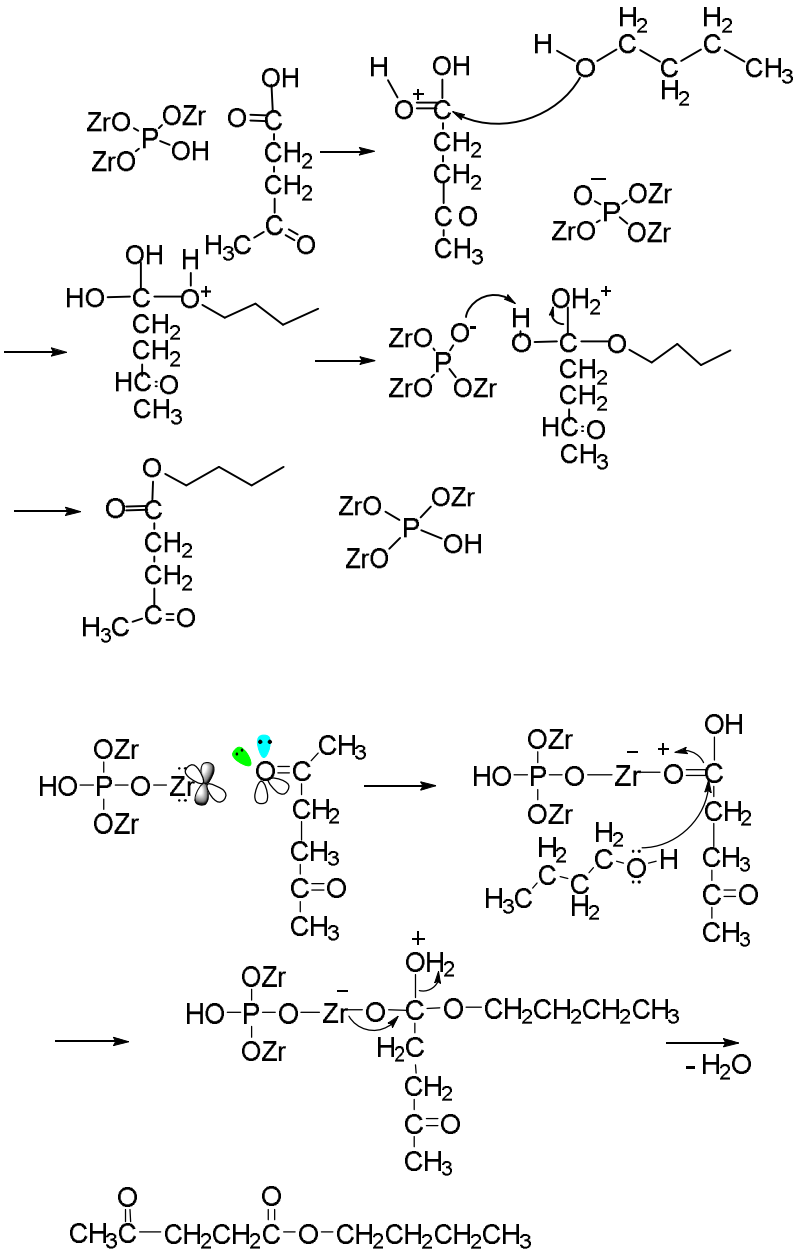

Scheme 2. Mechanism of conversion of levulinic acid to n-butyl levulinate (Path A top, path B below)

to the data, m-ZrP-2 has the best activity due to its maximum P-OH group concentration and acidic properties. The total acidity (Brönsted and Lewis acidity) of the m-Zrps increases gradually with increasing phosphate loading [39]. Hence, the efficiency of m-ZrP-2 was higher than m-ZrP-1.5 with the lower ratio of phosphate added. However, an additional increase of phosphate probably causes polyphosphate to form and as a result reduced the acidity and yield. m-ZrO_2 with no phosphate has the least acidity and efficiency.

The influence of reaction temperature on conversion of levulinic acid to n-butyl levulinate. The effect of temperature on the conversion of levulinic acid to butyl

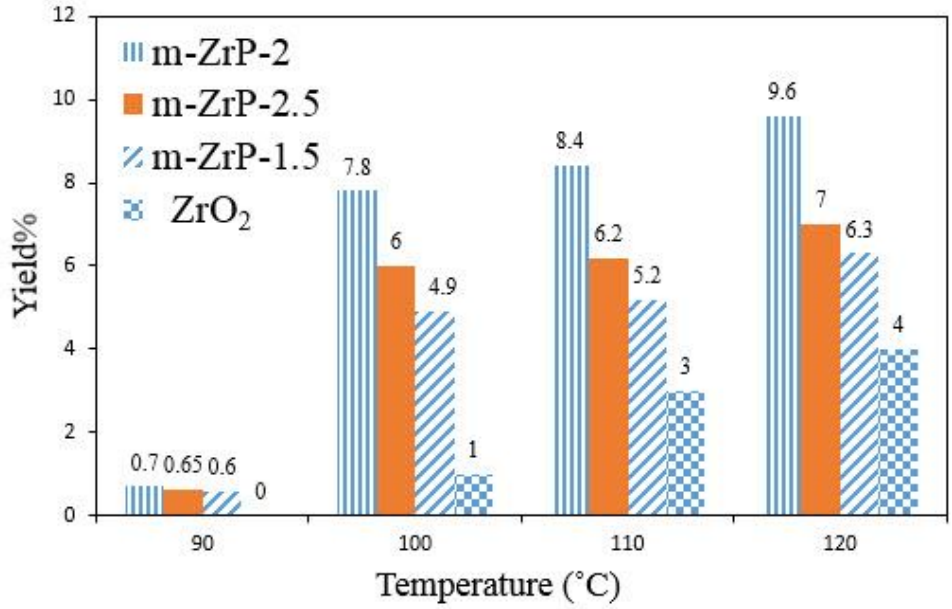

Fig. 5. Influence of the phosphate content on the catalytic activity. Reaction conditions: 0.5 mL LA (0.572 g); 4.5 mL n-butanol (3.645 g) and 0.05 g catalyst; reaction time, 2 h.

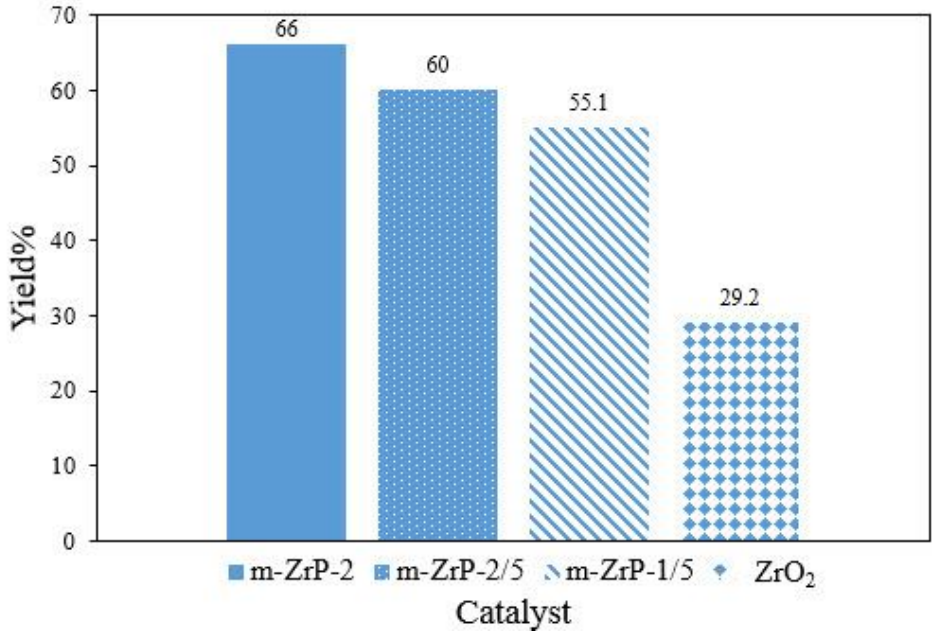

Fig. 6. Influence of the phosphate content on the catalytic activity. Reaction conditions: 0.5 mL LA (0.572 g); 4.5 mL n-butanol (3.645 g) and 0.05 g catalyst; temperature, 120 °C; reaction time, 7 h.

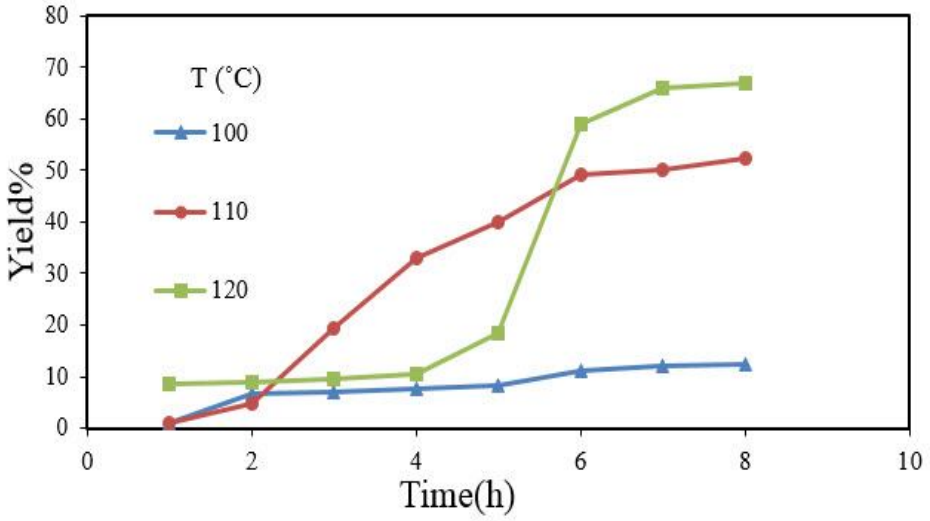

Fig. 7. Influence of the reaction time and temperature on the reaction yield. Reaction conditions: 0.5 mL LA (0.572 g); 4.5 mL n-butanol (3.645 g) and 0.05 g catalyst.

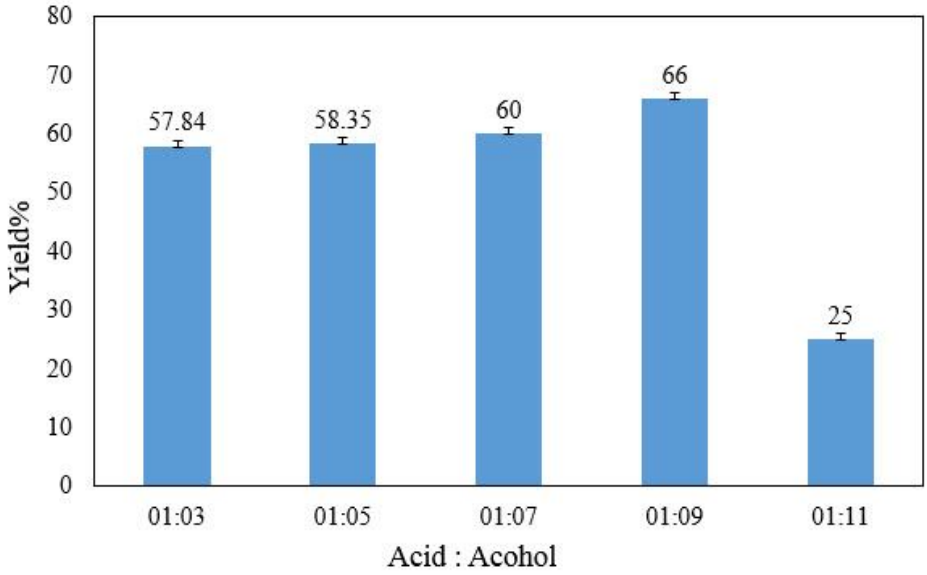

Fig. 8. Influence of LA/n-butanol ratio on the reaction yield. Reaction conditions: 0.05 g catalyst; temperature, 120 °C; reaction time, 7 h.

levulinate by m-ZrP-2 catalyst was investigated and the results are presented in Fig. 7. As can be seen, with increasing temperature from 100-120 °C, the yield of reaction increased to 66% whereas no increase in yield was noticed higher than 120 °C that could justify that butyl alcohol evaporation.

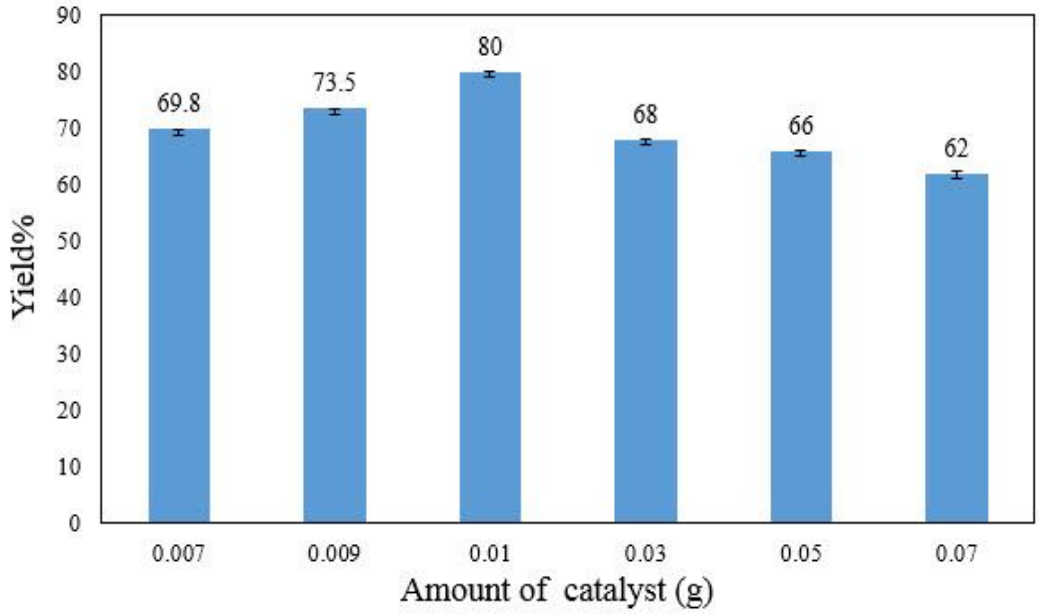

Fig. 9. Influence of the catalyst weight on the reaction yield. Reaction conditions: 0.5 ml LA (0.572 g); 4.5 mL n-butanol (3.645 g); temperature, 120 °C and reaction time, 7 h.

Influence of the reaction time on conversion of levulinic acid to n-butyl levulinate. The effect of reaction time was examined and showed that the BL yield increased during the increasing reaction time until 7 h (Fig. 7). After 8 h of reaction started, the yield no changed, probably as a result of blocking of active sites with water molecules generated during the reaction which lead to deactivation of them. Therefore, 7 h was selected as the optimum reaction time.

Influence of the ratios of LA/n-butanol on the conversion of levulinic acid to n-butyl levulinate. The influence of various LA/n-butanol ratios on the conversion of LA to BL is plotted in Fig. 8. It can be seen that increasing LA/n-butanol ratio from 1:3 to 1:9 leads to a rise in the reaction yield from 57.84 to 66% and then a decrease at higher alcohol added. It could be a consequence of the occupation of the active sites of the catalyst with additional n-butanol and dilution of the mixture. Therefore, the optimal LA/n-butanol ratio of 1:9 was chosen as the best in the research.

The effect of the catalyst weight on esterification of LA to BL. Esterification of LA to BL was carried out at different weights of m-ZrP-2 catalyst concerning levulinic acid (Fig. 9). The efficiency of catalyst increased by increasing catalyst amount because, at higher catalyst weight, more active sites were available. Enhancing the catalyst weight leads to a decrease in BL yield due to catalyst agglomeration or decrease contact opportunities between the reactants. The maximum BL yield was obtained using 0.01 g catalyst loading therefore, this value was chosen for the esterification of LA to BL.

The recycling and reusability of the catalyst. The long-term stability and reusability of a catalyst is an important factor in its efficiency (Fig. 10). Accordingly, recycled m-ZrP-2 catalyst was constantly used in six reactions under the same conditions. For this purpose, after completion of the reaction, the catalyst was separated by filtration, washed with deionized water and acetone, and finally dried in the oven. As seen in Fig. 11, the BL yield decreases about 2% from the first to the sixth cycle that may be due to the blocking of the active sites of the catalyst by the products which cannot be removed simple. XRD of the recycled catalyst presented in Fig. 11, which indicated the mesoporous structure of the catalyst.

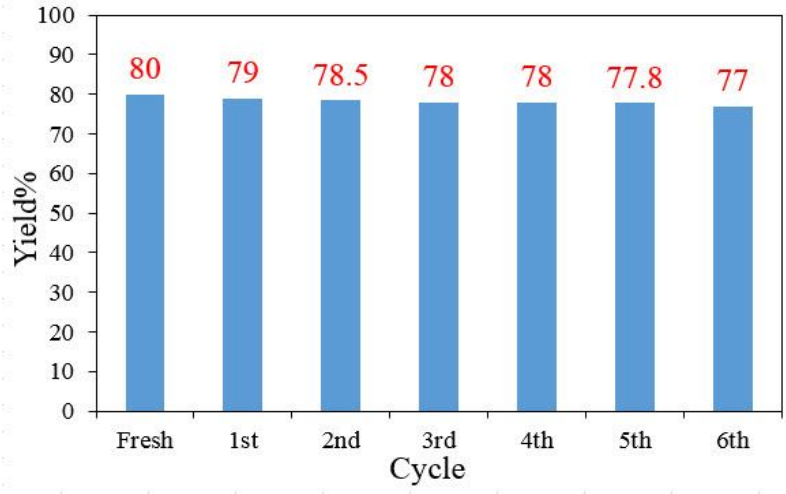

Fig. 10. n-BL yield as a function of the run times of catalyst. Reaction conditions: 0.5 mL LA (0.572 g); 4.5 mL n-butanol (3.645 g); 0.05 g catalyst; temperature, 120 °C and reaction time, 7 h.

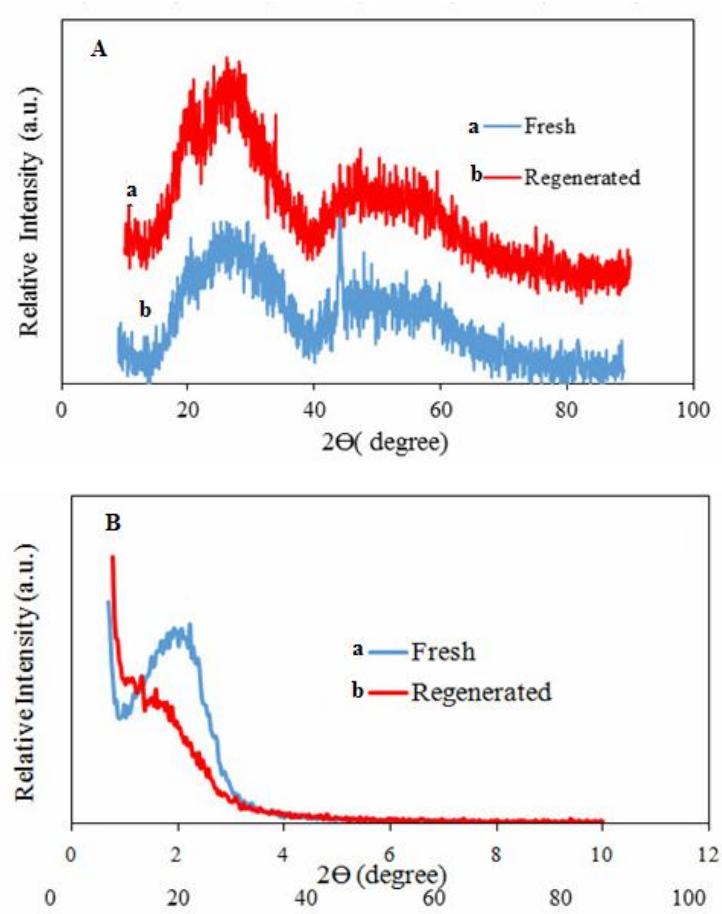

Fig. 11. Wide angle (A) and small angle (B) XRD patterns of synthesized m-ZrP-2.

CONCLUSIONS

In conclusion, three types of mesoporous zirconium phosphate catalysts with the different molar ratio of phosphate to Zirconium were synthesized and used to the esterification of levulinic acid to n-butyl levulinate. Their catalytic activity compared and it was observed that among the catalysts, the m-ZrP-2 catalyst showed the best efficiency in the reaction with an 80% yield due to its high acidity. The optimum reaction conditions were found to be 120 ºC and 8 h. The catalyst was recycled and reused six times in the same conditions. According to the results, significant changes in reaction efficiency were not observed.

ACKNOWLEDGMENTS

We would like to thank Isfahan University of Technology (IRAN) for financial support (Research Council Grant).

REFERENCES

[1] C.O. Tuck, E. Pérez, I.T. Horváth, R.A. Sheldon, M. Poliakoff, Science 337 (2012) 695.
[2] J.J. Bozell, G.R. Petersen, Green Chem. 2010, 12, 539
[3] G.W. Huber, S. Iborra, A. Corma, Chem. Rev. 106 (2006) 4044.
[4] Z. Babaei, A.N. Chermahini, M. Dinari, M. Saraji, A. Shahvar, Sustainable Energy Fuels 3 (2019) 1024.
[5] G. Centi, P. Lanzafame, S. Perathoner, Catal. Today 16 (72011) 14.
[6] F.D. Pileidis, M. Titirici, Chem.Sus. Chem. 9 (2016) 562.
[7] B. Girisuta, L. Janssen, H.J. Heeres, Ind. Eng. Chem. Res. 46 (2007) 1696.
[8] S. Kumaravel, S. Thiripuranthagan, R. Radhakrishnan, E. Erusappan, M. Durai, A. Devarajan, A. Mukannan, J. Nanosci. Nanotechnol. 19 (2019) 6965.
[9] E. Lotero, Y. Liu, D.E. Lopez, K. Suwannakarn, D.A. Bruce, J.G. Goodwin, Ind. Eng. Chem. Res. 44 (2005) 5353.
[10] E. Christensen, A. Williams, S. Paul, S. Burton, R.L. McCormick, Energ. Fuel 25 (2011) 5422.
[11] J.R. Kean, A.E. Graham, Catal. Commun. 59 (2015) 175.
[12] F.G. Cirujano, A. Corma, F.X.L. Xamena, Chem. Eng. Sci. 124 (2015) 52.
[13] L. Peng, X. Gao, K. Chen, Fuel. 160 (2015) 123.
[14] A. Corma, Chem. Rev. 95 (1995) 559.
[15] T. Okuhara, Chem. Rev. 102 (2002) 3641.
[16] Y. Kuwahara, T. Fujitani, H. Yamashita, Catal. Today 237 (2014) 18.
[17] D. Song, S. An, Y. Sun, Y. Guo, J. Catal. 333 (2016) 184.
[18] S.B. Onkarappa, M. Javoor, S.S. Mal, S. Dutta, Chem. Select 4 (2019) 2501.
[19] D.R. Fernandes, A.S. Rocha, E.F. Mai, C.J.A. Mota, V.T. Da Silva, Appl. Catal. A Gen. 425 (2012) 199.
[20] M.A. Tejero, E. Ramírez, C. Fité, J. Tejero, F. Cunill, Appl. Catal. A Gen. 517 (2016) 56.
[21] S. Dharne, V.V. Bokade, J. Nat. Gas Chem. 20 (2011) 18.
[22] S.S.R. Gupta, M.L. Kantam, Catal. Commun. 124 (2019) 62.
[23] A. Taguchi, F. Schüth, Micropor. Mesopor. Mat. 77 (2005) 1.
[24] S. Soltani, U. Rashid, S.I. Al-Resayes, I.A. Nehdi, Mesoporous Catalysts for Biodiesel Production: A New Approach, in: Clean Energy Sustain. Dev., Elsevier, 2017, p. 487.
[25] E. Mannei, F. Ayari, E. Asedegbega-Nieto, M. Mhamdi, G. J. Iran. Chem. Soc. 17 (2020) 1087.
[26] A.N. Chermahini, M.K. Omran, H.A. Dabbagh, G. Mohammadnezhad, New J. Chem. 39 (2015) 4814.
[27] F. Mumtaz, M.F. Irfan, M.R. Usman, J. Iran. Chem. Soc. (2021), DOI: Ñ0.1007/s13738-021-02183-2.
[28] K. Niknam, H. Hashemi, M. Karimzadeh, D. Saberi, J. Iran. Chem. Soc. 17 (2020) 3095.
[29] F. Ahmadian, A.R. Barmak, E. Ghaderi, M. Bavadi, H. Raanaei, K. Niknam, J. Iran. Chem. Soc. 16 (2019) 2647.
[30] N. Pasha, N. Lingaiah, R. Shiva, Catal. Lett. 149 (2019) 2500.
M.P. Pachamuthu, V.V. Srinivasan, R. Karvembu, R. Luque, Micropor. Mesopor. Mat. 287 (2019) 159.
[31] M.M. Tabrizi, A.N. Chermahini, Z. Mohammadbagheri, J. Environ. Chem. Eng. 7 (2019) 103420.

[32] A.N. Chermahini, M. Nazeri, Fuel Process. Technol. 167 (2017) 442.
[33] A.N. Chermahini, M. Assar, J. Iran. Chem. Soc. 16 (2019) 2045.
[34] D. Song, P. Zhang, Y. Sun, Q. Zhang, Y. Guo, Micropor. Mesopor. Mat. 279 (2019) 352.
[35] A. Sinhamahapatra, N. Sutradhar, B. Roy, A. Tarafdar, H.C. Bajaj, A.B. Panda, Appl. Catal. A Gen. 385 (2010) 22.
[36] A. Jain, A.M. Shore, S.C. Jonnalagadda, K.V. Ramanujachary, A. Mugweru, Appl. Catal. A Gen. 489 (2015) 72.
[37] K.N. Rao, A. Sridhar, A.F. Lee, S.J. Tavener, N.A. Young, K. Wilson, Green Chem. 8 (2006) 790.
[38] A. Sinhamahapatra, N. Sutradhar, S. Pahari, H.C. Bajaj, A.B. Panda, Appl. Catal. A Gen. 394 (2011) 93.
[39] C.A. Emeis, J. Catal. 141 (1993) 347.
[40] H.-N. Kim, S.W. Keller, T.E. Mallouk, J. Schmitt, G. Decher, Chem. Mater. 9 (1997) 1414.
[41] B. Chakraborty, B. Viswanathan, Catal Today 49 (1999) 253.
[42] E. Siva Sankar, G.V. Ramesh Babu, K. Murali, B. David Raju, K.S. Rama Rao, RSC Adv. 6 (2016) 20230.